EXTREME shearography

High-speed shearography instrument for in-plane surface strain measurements during an impact event

Anisimov, Andrei G.; Groves, Roger M.

DOI
10.1117/12.2525801

Publication date
2019

Document Version
Final published version

Published in
Optical Measurement Systems for Industrial Inspection XI

EXTREME shearography: high-speed shearography instrument for in-plane surface strain measurements during an impact event

Anisimov, Andrei, Groves, Roger

Andrei G. Anisimov, Roger M. Groves, "EXTREME shearography: high-speed shearography instrument for in-plane surface strain measurements during an impact event," Proc. SPIE 11056, Optical Measurement Systems for Industrial Inspection XI, 110560J (21 June 2019); doi: 10.1117/12.2525801

SPIE.

Event: SPIE Optical Metrology, 2019, Munich, Germany

EXTREME shearography: high-speed shearography instrument for in-plane surface strain measurements during an impact event

Andrei G. Anisimov*, Roger M. Groves
Aerospace Non-Destructive Testing Laboratory, Delft University of Technology,
Kluyverweg 1, 2629 HS, Delft, The Netherlands

ABSTRACT

This work presents the design and the latest experimental results on the surface strain measurements during an impact event obtained with the EXTREME high-speed shearography instrument. The shearography technique is used in this project to provide a quantitative measurement of the surface strain development at the first moments of the impact event (μs time scale) which may reveal the initiation of the failure mechanisms in composite materials. Experimentally measured surface strain components over the field of view will be used as input and validation data for new numerical and analytical models of the impact response of composites. The new configuration of the shearography instrument realises measurements of the in- and out-of-plane surface strain components to improve coupling with the numerical models. Two viewing directions (shearing interferometers) with a double-frame approach are used to capture the interferograms during the impact. The interferometers realise a double-imaging Mach-Zehnder scheme for the spatial phase-shifting with independent control of the shearing amount and the carrier frequency. The set of technical parameters of the developed shearography instrument makes it one of the most extreme applications of shearography for material characterisation. The framework for this work is the "EXTREME Dynamic Loading – Pushing the Boundaries of Aerospace Composite Material Structures" Horizon 2020 project.

Keywords: high-speed shearography, double-pulse shearography, flexural waves, impact, composite materials, surface strain

1 INTRODUCTION

Composite materials are vulnerable to extreme dynamic loadings such as blade off events or foreign object damage (hail, runway debris, bird strike)[1]. Improving the impact response of composite materials is an important direction of the materials development when the risk of the impact is high, e.g. for the leading edges of an aircraft. The strain development during the impact is of particular interest for both materials modelling and experimental researchers[2,3]. The shearography[4-6] (speckle pattern shearing interferometry) technique is used in this project to provide a quantitative measurement of the surface strain development at the first moments of the impact event (μs time scale) which may reveal the initiation of the failure mechanisms in metals and composite materials. When shearography is used for monitoring of dynamic events, the phase corresponding to the deformation of the object can be extracted from each captured interferogram by using a spatial phase shift[7] with Mach-Zehnder[8] or Michelson interferometers[9].

This work presents the design and recent results on the EXTREME shearography development with the analysis of the in- and out-of-plane surface strain components, which is a continuation of the previously reported results[10] when only the out-of-plane surface strain components were measured. The previous paper[10] also includes the literature overview of the application of shearography and speckle interferometry techniques to vibration and impact monitoring. The previous configuration[10] of the shearography instrument realised measurements of the out-of-plane surface strain components ($\partial w/\partial x$, $\partial w/\partial y$) during the impact using the double frame approach. The spatial phase shift was based on a modified Michelson interferometer with 4f system. Then the interdependence of the interferometer parameters resulted in a relatively large shear distance which was not suitable for the dynamic event with high strain values.

The new configuration of the shearography instrument realises measurements of the in- and out-of-plane surface strain components during the impact using the double frame approach and a double imaging Mach-Zehnder interferometer[11,12]. The main criteria for the continuation of the development were derived by maximising the value of the expected results for the validation of numerical models – to measure both in- and out-of-plane surface strain components at impact speeds up to 200 m/s with a temporal resolution up to sub-μs over the field of view of 100×100 mm.

*a.g.anisimov@tudelft.nl; phone +31 15 27 83099; http://www.aerondt.tudelft.nl

Optical Measurement Systems for Industrial Inspection XI, edited by Peter Lehmann, Wolfgang Osten, Armando Albertazzi Gonçalves Jr., Proc. of SPIE Vol. 11056, 110560J · © 2019
SPIE · CCC code: 0277-786X/19/$21 · doi: 10.1117/12.2525801

The framework for this work is the "EXTREME Dynamic Loading – Pushing the Boundaries of Aerospace Composite Material Structures" Horizon 2020 project[13]. Within the project, the shearography data is fused with high-speed 3D digital image correlation[14] (DIC) and in-situ impact data from fibre optical sensors based on Fibre Bragg Gratings (FBG), embedded and surface mounted piezo-electric sensors[15]. This fusion uses the strong points of each technique to provide reliable experimental input for developing numerical and analytical models of composites.

2 HIGH-SPEED MULTICOMPONENT SHEAROGRAPHY

A multicomponent shearography is needed when the in-plane surface strain has to be assessed during a dynamic event[5]. A general solution for that is a 3D shearography configuration capable of decoupling the surface strain components e.g. with 3 shearing cameras[5]. Due to the complexity of the EXTREME shearography instrument[10], only 2 shearing cameras are used in this project with a configuration sensitive to the in- and out-of-plane components and excluding the shear strain.

A schematic of the EXTREME shearography instrument is presented in Figure 1. A speckle pattern is produced by illuminating a specimen with an expanded laser beam through an additional diffuser. Interferograms are recorded with two symmetrically placed shearing cameras at the initial moment of the impact (from 0 to 10 μs after the impact). Each camera records a pair of interferograms which are synchronised with the laser pulses[16]. Later the surface strain which was built up in between two laser pulses is processed. In this project, the object is deformed by the impact loading with a gas-gun using an impactor. The synchronisation is done in a real-time to obtain a reliable registration of the impact event.

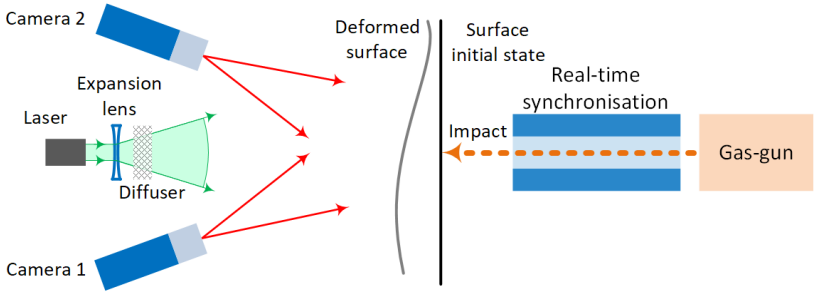

Figure 1. The EXTREME shearography instrument for in- and out-of-plane measurements.

The shearography configuration for one of the cameras with spatial shifting using the double imaging Mach-Zehnder interferometer[11] is presented in Figure 2 (a). The interferometer was modified by using a pair of slits instead of circular apertures to improve the energy efficiency and quality of the revealed phase maps[17]. The slits are geometrically shifted from the joint optical axis to define the carrier frequency Figure 2 (b). The corresponding data processing flow is presented in Figure 2 (c).

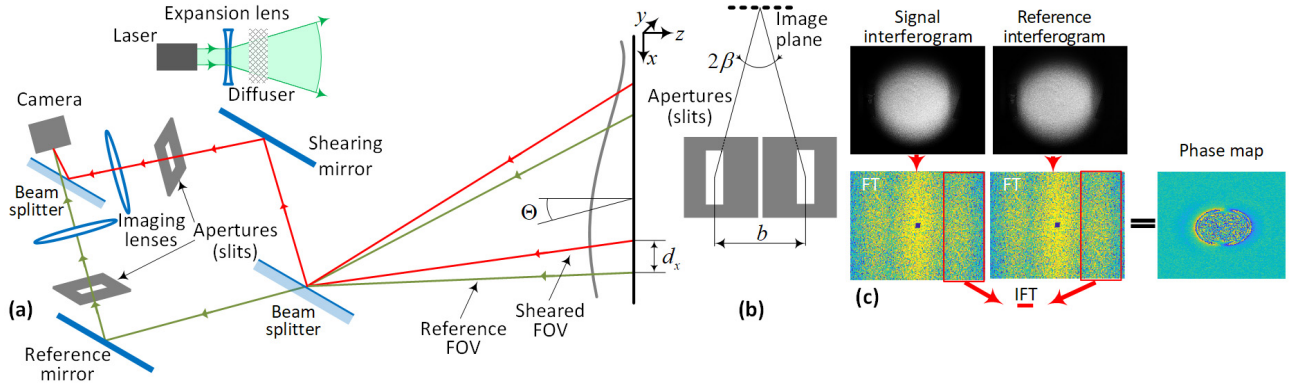

Figure 2. Modified double imaging Mach-Zehnder interferometer for one measurement channel: (a) schematic representation of the optical paths in the shearing device, (b) relative off-axis offset of the slits and (c) data processing flow in the Fourier domain (FOV – field of view, FT – Fourier transform, IFT – inverse Fourier transform).

When 2 shearing cameras are used, each of them will provide phase changes $\Delta\phi_{xj}$ (camera number $j = 1, 2$) which can be extracted from the Fourier side-spectra of the recorded interferograms. If the illumination and viewing directions are in the xz-plane and a relatively small shear distance d_x is applied in the x-direction, the phase change $\Delta\phi_x$ becomes a function of the in- and out-of-plane surface strain components ($\partial u/\partial x$ and $\partial w/\partial x$, respectively) with a sensitivity to the shear strain $\partial v/\partial x$ close to 0:

$$\Delta\phi_x = \phi'_x - \phi_x^{ref} = \frac{2\pi}{\lambda}\left(k_x\,\partial u/\partial x + k_y\,\partial v/\partial x + k_z\,\partial w/\partial x\right)d_x \overset{\text{if in } xz\text{-plane}}{\approx} \frac{2\pi}{\lambda}\left(k_x\,\partial u/\partial x + k_z\,\partial w/\partial x\right)d_x, \quad (1)$$

where ϕ'_x and ϕ_x^{ref} are the signal and reference phase differences obtained before and after deformation, λ is the laser wavelength, $(k_x\ k_y\ k_z)$ – components of the sensitivity vector, that is the bisector of the viewing angle Θ between the illumination and viewing directions[5]. The surface strain components $\partial u/\partial x$ and $\partial w/\partial x$ for the shear d_{xj} in the x-direction can be calculated[5] by processing the phase changes $\Delta\phi_{xj}$ obtained at each camera $j = 1, 2$:

$$\begin{bmatrix}\partial u/\partial x\\ \partial w/\partial x\end{bmatrix} = \frac{\lambda}{2\pi}\begin{bmatrix}k_{x1} & k_{z1}\\ k_{x2} & k_{z2}\end{bmatrix}^{-1}\begin{bmatrix}\Delta\phi_{x1}/d_{x1}\\ \Delta\phi_{x2}/d_{x2}\end{bmatrix} \overset{\text{if symmetric setup in } xz\text{-plane}}{\approx} \frac{\lambda}{4\pi}\begin{bmatrix}1/\sin(\Theta) & 1/\sin(-\Theta)\\ 1/(\cos(\Theta)+1) & 1/(\cos(\Theta)+1)\end{bmatrix}\begin{bmatrix}\Delta\phi_{x1}/d_{x1}\\ \Delta\phi_{x2}/d_{x2}\end{bmatrix}. \quad (2)$$

The surface strain components in the y-direction ($\partial u/\partial y$, $\partial w/\partial y$) can be calculated in the same way[5] replacing x by y in Equations (1, 2). For accurate strain estimation, the first part of Equations (1) has to be used with an implementation of the sensitivity vector corrections and the shear calibration over the field of view. In addition, the actual camera's coordinates have to identified by the cameras geometric calibration, e.g. as a stereo pair[18].

In case of the spatial phase shift with the double imaging Mach-Zehnder interferometer[11] used for the optical arrangement (Figure 2), the slits act as a low-pass filters that limit the frequency bandwidth of the recorded interferogram with the cut-off frequency[8] $f_c = D/2\lambda f$, where D is the slit width projected to the focal plane, f is the focal length of the imaging lens. The offset (carrier) frequency is independently set[11] by the angular offset of the slits β as $f_o = \sin\beta/\lambda$. In order to isolate these maximums, the offset frequency f_o has to be at least twice higher than f_c, i.e. $2f_c \le f_o \Rightarrow D \le f\sin\beta$. Normally the focal length f is the least flexible parameter as it is defined by the desired field of view, the instrument geometry and the camera sensor size.

Another restriction is the dynamic range of the measuring strain which has to be maximized for each impact event. For that, the shear distance typically has to be decreased. It was found experimentally that the shear distance should be more than 2 speckle sizes for reliable phase retrieval. To minimize the subjective speckle size $\Delta s = \lambda f/D$, the slit width D was maximized. However, the minimum speckle size Δs has to be more than 6 pixels[8]. The trade-off for the slit width D can be written as:

$$\lambda f/6p_x \le D \le f\sin\beta, \quad (3)$$

where p_x is the pixel size in x-direction. In addition, the camera pixel size and the number of pixels define the highest spatial frequency and the frequency range, respectively. Therefore, for reliable spectrum separation, it is preferable to use the sensors with the minimal pixel size and the highest spatial resolution.

3 EXPERIMENTAL RESULTS

3.1 EXTREME shearography instrument for in- and out-of-plane surface strain measurements

The modified configuration of the shearography instrument (Figure 3) realises measurements of the in- and out-of-plane surface strain components ($\partial u/\partial x$ and $\partial w/\partial x$ or $\partial v/\partial y$ and $\partial w/\partial y$ depending on the shear direction) during the impact using the double frame approach. The chamber has 3 zones: an impact zone with the synchronisation unit, a monitoring zone where the back surface of the specimen is observed and a shearography zone with the shearing cameras. The gas-gun is adapted for impact speeds up to 200 m/s with pressurised air or nitrogen.

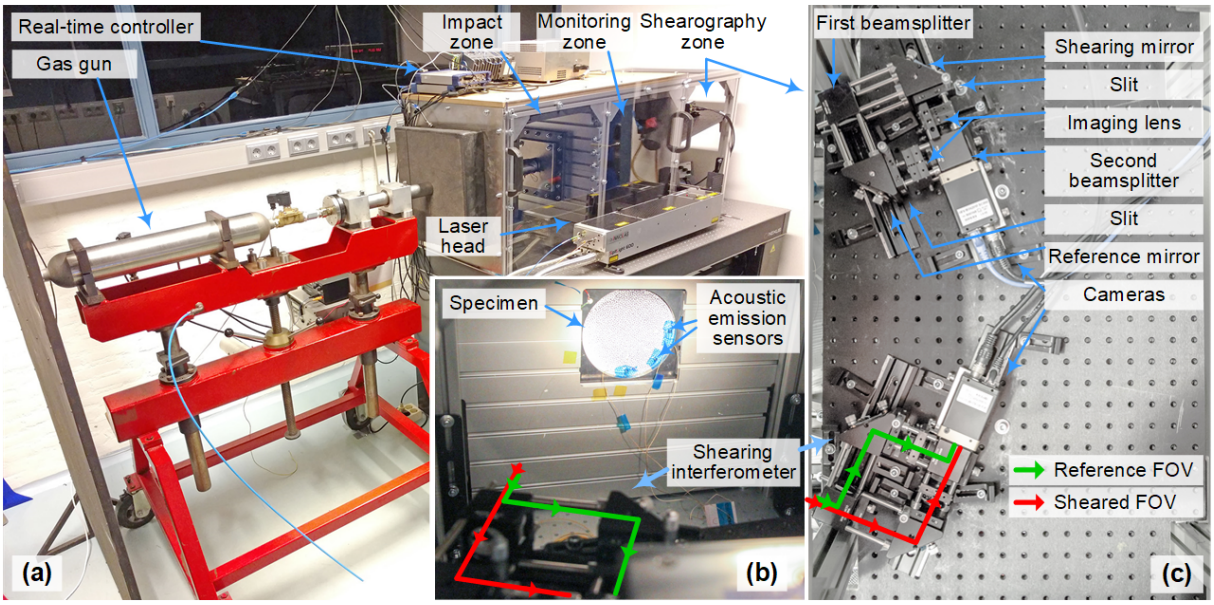

Figure 3. EXTREME shearography instrument for in- and out-of-plane surface strain measurements: (a) overview of the instrument, the gas-gun and the impact chamber, (b) the monitoring zone as seen from one of the shearing interferometers, (c) two symmetric shearing interferometers implementing the double-imaging scheme.

Each double-imaging Mach-Zehnder interferometer[11] consists of a double-frame camera BOBCAT B3420 by Imperx. The camera has an interline frame transfer with a resolution of 3388×2712 pixels, a pixel size of 3.69x3.69 μm and an interframing time of 200 ns. The speckle pattern is produced by illuminating the field of view of 120×120 mm with an expanded beam from a pulsed laser in a double pulse regime (customised SpitLight 600 Nd:YAG-Lasersystem by InnoLas Laser GmbH, wavelength 532 nm). An additional ground glass diffuser (Figure 1) is used to normalise the energy distribution over the illuminated area to overcome the initial circular fringes in the beam due to complex modes combination. Two portions of the single pulse with energy from 100 up to 500 mJ sequentially illuminate the object under the control of a Pockels cell with the minimum separation time of 1 μs. The synchronisation in real-time is based on the approaching impactor using a set of 20 optical interrupters which results in a reliable prediction of the impact event with the accuracy up to 1 μs[10]. In each interferometer, two slits were placed at the front focal planes of the imaging lenses to achieve a better quality of the phase maps in comparison with a circular aperture[17]. The trade-off between the interferometer parameters (Equation 3) was made as follows:

a) the distance between the camera and the object of 500-600 mm was based on safety measures;
b) the focal length was maximised up to 50 mm (Xenoplan 2.8/50 by Schneider) and was also defined by the specimen size of 200×200 mm with the visible area of Ø150 mm;
c) each slit was shifted from the joint axis by 1.9 mm (β=2.3°) resulting in the offset frequency close to a half of the maximum one, see Figure 2 (b, c);
d) the 1.8 mm slit was chosen as a rational compromise resulting in the absence of the overlap of the central and side maximums of the Fourier spectra and the average subjective speckle size of 7 pixels (corresponding to 0.35 mm; along with the x-axis).
e) the shear distance d_x was set at 17 to 21 pixels (0.9..1.1 mm) and calibrated over the field of view for both cameras as in[10] by processing a checkerboard image captured through the reference and the sheared field of views.

3.2 Experimental in- and out-of-plane strain components maps

The in- and out-of-plane surface strain components were measured during impact tests on 4 mm thick 6082-T6 aluminium specimens (Figure 4) and 3 mm thick carbon fibre reinforced composite (CFRP) specimens with 0/90/0/90/0 layup of unidirectional plies (Figure 5). The impactor and the damage in the CFRP specimen are shown in Figure 6. No penetration of the impactor was observed. For the aluminium specimen, repeatable indentations were measured. During the tests, the impactor speed was in the range of 58.5±0.5 m/s corresponding to a 53.8..55.7 J impact energy range with an impactor of 32 g (Figure 6 (c)).

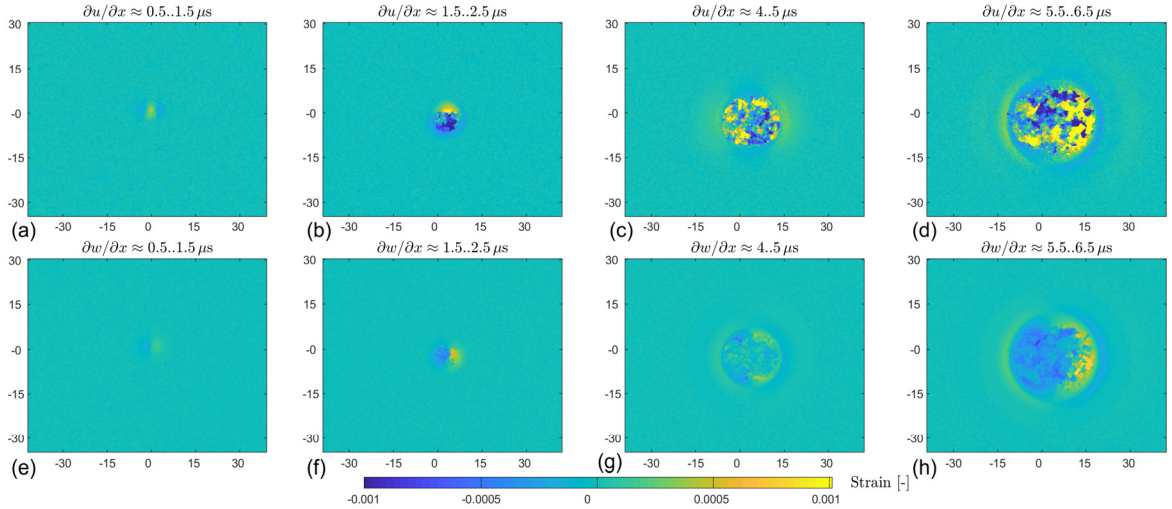

Figure 4. In- and out-of-plane surface strain maps ($\partial u/\partial x$ and $\partial w/\partial x$) of 4 mm aluminium plates (6082-T6) at the time from 0 to 5.5..6.5 µs after the impact (axes units mm).

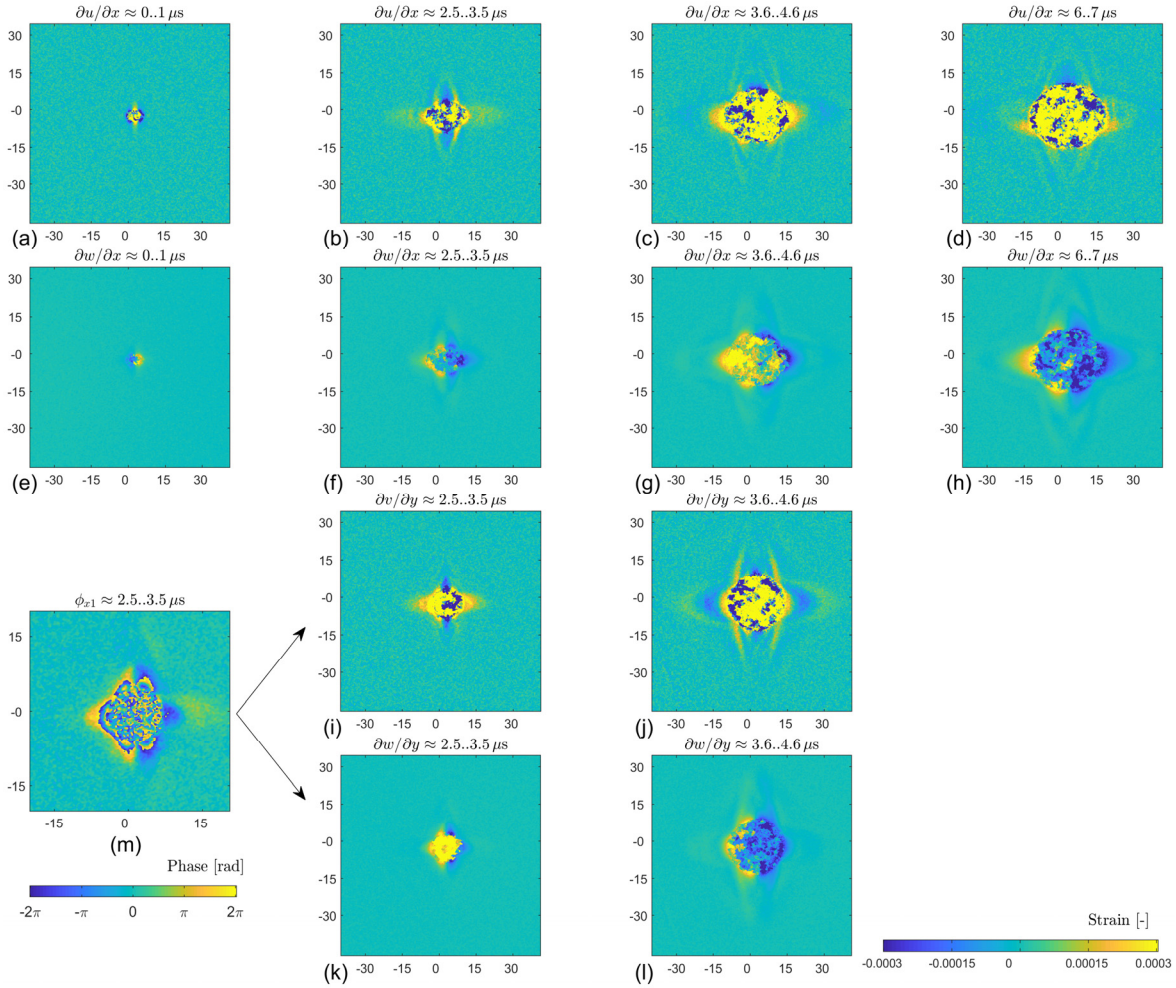

Figure 5. In- and out-of-plane surface strain maps ($\partial u/\partial x$ and $\partial w/\partial x$, $\partial v/\partial y$ and $\partial w/\partial y$) of 3 mm CFRP specimens at the time from 0 to 6..7 µs after the impact (axes units mm) with an additional zoom into the unwrapped phase map (m).

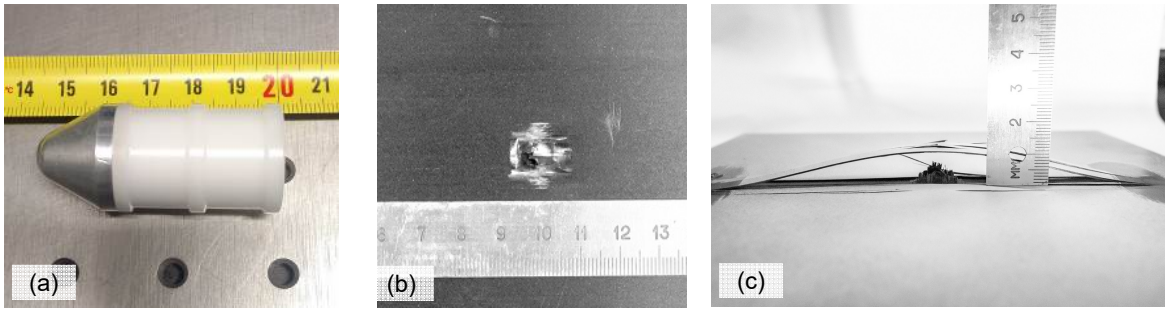

Figure 6. The impactor (a) and (b, c) the damaged in 3 mm CFRP specimen after the impact.

The strain maps reveal the evolution of $\partial u/\partial x$ and $\partial w/\partial x$ during 1 μs with varying delay up to 7 μs starting from the moment of the impact. This delay was estimated with an accuracy of ±0.5 μs by matching the acoustic emission signals from the piezo sensors with the laser pulses and the wave propagation delay from the impact location to the acoustic emission sensors[10]. Note that in some cases the phase unwrapping algorithm has not been able to fully identify all the phase steps. Each impact experiment with a new specimen resulted in a pair of maps ($\partial u/\partial x$ and $\partial w/\partial x$) presented in columns in Figures 4 and 5, e.g. Figure 4 (a, e). Strain components $\partial v/\partial y$ and $\partial w/\partial y$ in Figure 5 were measured by rotating the specimens by 90 degrees and keeping the same calibrated shear distance d_x.

4 DISCUSSION

The first strain maps in Figures 4 (a, b, e, f) and 5 (a, e) reveal the elastic response of the material during the initiation of the impact event during the first 0..2 μs after the impact. Further in time (from 2.5 to 7 μs) the initiation and propagation of the flexural wave is observed at varying delays after the impact. Previously[10] it was shown that the observed flexural waves travel with the speed corresponding to the wave velocity of the longitudinal ultrasonic wave (velocity varies for aluminium alloys in the range of 6200..6300 m/s). For the aluminium specimens (Figure 4), the expected symmetric propagation of the waves was observed. The wavefront for the composite specimens (Figure 5) reveals the anisotropy of the material properties resulting in different wave velocities in different directions. The waves travel faster along the fibre directions (vertical and horizontal) and slower in diagonal directions[19,20].

The main problem of the strain maps and phase maps in the previous work[10] was the loss of the measurement results in impact location after 3-4 μs depending on the material properties. This happens because of a high number of fringes at the impact location in characteristic butterfly pattern. Figure 5 (m) shows the filtered wrapped phase map from one of the cameras. Later the unresolved fringes are clustered during the unwrapping procedure which results in the presented central parts of the strain maps. The overall dynamic range of the presented Mach-Zehnder scheme is significantly improved in comparison with the previous Michelson configuration[10]. However, further improvements are limited to:

a) increasing the laser wavelength from 532 nm to 1064 to double the dynamic range of the recording surface strain, which will also half the speckle size with the current focal length (50 mm) and the slit width (1.8 mm);
b) increasing the focal length of the imaging lenses to increase the spatial resolution (Equation 3).

The peculiarity of the double imaging Mach-Zehnder interferometer[11] in comparison with the Michelson scheme[7,9] is in the beam splitter that has to be placed behind the imaging lenses (Figure 2 (a)) resulting in optical design difficulties in use of standard C/CS mount objective lenses and lenses with short focal lengths (less than 30 mm), using standard C/CS mount cameras for machine vision and optical metrology. The gap between the last mechanical part of the objective lens and the image plane of the camera sensor has to be at least 16.7 mm which corresponds to the reduced thickness of a 1 inch prism in air. When additional margins for the mechanical assembly, in practice 10-20 mm are taken into account, this results in a required gap of more than 30 mm. This makes most of the standard C-mount objective lenses not applicable for this task. Single lenses with the focal length of more than 25-30 mm can be used with the expected poor image quality. The objective lens used in this project (Xenoplan 2.8/50 by Schneider) together with the camera (BOBCAT B3420 by Imperx) have high integration capability by partial disassembly of the parts which does not affect the image quality.

The validation plan for the EXTREME shearography Figure 7 includes joint measurements with a high-speed 3D DIC instrument[14] developed in Ghent University, Belgium and the aforementioned piezo sensors[15] (step 1 in Figure 7). Then

the experimental results together with the post-impact inspection of the specimens (incl. damage area, indentation) will be used to validate the finite element model (FEM) developed by the University of Patras (steps 2, 3). At the final step, the modelled results will be compared with the shearography results.

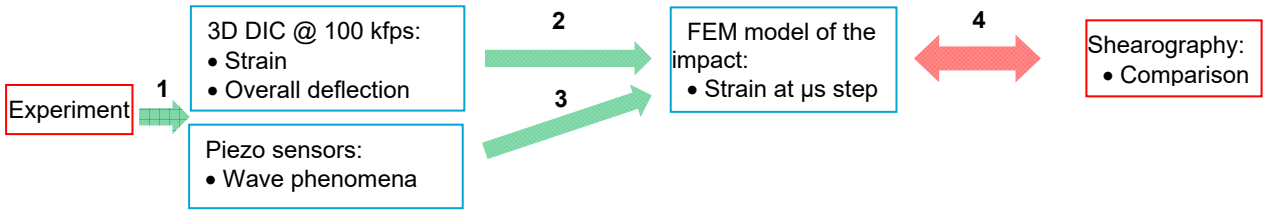

Figure 7. Validation plan for the EXTREME shearography.

5 CONCLUSIONS

The main value of the presented experimental results is in the μs mapping of the flexural waves during the impact with a symmetrical distribution for metals and an asymmetrical wave pattern for the composite materials. The measured anisotropy will be used as input and validation data for new numerical and analytical models of the impact response of composites and for validation of other experimental techniques as acoustic emission. Currently, the EXTREME shearography instrument realises measurements of the in- and out-of-plane surface strain components during the impact using the double frame approach. The overall set of technical parameters of the developed shearography instrument makes it one of the most extreme applications of shearography for material characterisation.

Future steps of the instrument development include optimisation of the interferometer to increase its dynamic range, exploring simultaneous measurements in multiple sharing directions[21] and recording of a sequence of interferograms (more than 2) in a "pulse train" regime.

ACKNOWLEDGEMENTS

The project "EXTEME" leading to this paper has received funding from the European Union's Horizon 2020 research and innovation program under agreement No. 636549.

REFERENCES

[1] Robin, O., "Mass criterion for wave controlled impact response of composite plates," Compos. Part A Appl. Sci. Manuf. 31(8) 879-887 (2000).
[2] Vignjevic, R., Djordjevic, N., De Vuyst, T. and Gemkow, S., "Modelling of strain softening materials based on equivalent damage force," Comput. Methods Appl. Mech. Eng. 335, 52-68 (2018).
[3] Giannaros, E., Kotzakolios, A., Sotiriadis, G., Tsantzalis, S. and Kostopoulos. V., "On fabric materials response subjected to ballistic impact using meso-scale modeling. Numerical simulation and experimental validation," Compos. Struct. 204, 745-754 (2018).
[4] Hung, Y. Y., "Shearography: a new optical method for strain measurement and non-destructive testing," Opt. Eng. 21, 213391 (1982).
[5] Steinchen, W. and Yang, L., [Digital Shearography], SPIE Press, Bellingham, Washington (2003).
[6] Francis, D., Tatam, R. P. and Groves, R. M., "Shearography technology and applications: a review," Meas. Sci. Technol. 21, 102001, 29 (2010).
[7] Yang, L. and Xie, X., [Digital Shearography: New Developments and Applications], SPIE Press, Bellingham, Washington (2016).
[8] Pedrini, G., Zou, Y. L. and Tiziani, H. J., "Quantitative evaluation of digital shearing interferogram using the spatial carrier method," Pure and Appl. Opt. A 5.3, 313 (1996).
[9] Xie, X., Yang, L., Xu, N. and Chen, X., "Michelson interferometer based spatial phase shift shearography," Appl. Opt. 52(17), 4063-4071 (2013).

[10] Anisimov, A. G., Groves, R. M., " EXTREME shearography: development of a high-speed shearography instrument for measurements of the surface strain components during an impact event," Proc. SPIE 10834, 108340X (2018).
[11] Gao, X., Yang, L., Wang, Y., Zhang, B., Dan, X., Li, J. and Wu, S., "Spatial phase-shift dual-beam speckle interferometry," Appl. Opt. 57(3), 414-419 (2018).
[12] Gao, X., Wang, Y., Dan, X., Sia, B. and Yang, L., "Double imaging Mach-Zehnder spatial carrier digital shearography," Journal of Modern Optics, J. Mod. Opt. 66(2), 153-160 (2019).
[13] "EXTREME Dynamic Loading – Pushing the Boundaries of Aerospace Composite Material Structures," www.extreme-h2020.eu (03 June 2019).
[14] Elmahdy, A., Verleysen, P., "Tensile behavior of woven basalt fiber reinforced composites at high strain rates," Polym. Test. 76, 207-221 (2019).
[15] De Simone, M. E., Cuomo, S., Ciampa, F., Meo, M., Nitschke, S., Hornig, A. and Modler, N., "Acoustic emission localization in composites using the signal power method and embedded transducers," Proc. SPIE 10971, 109711O (2019).
[16] Nösekabel, E. H., Honsberg, W. and Kelnberger, R., "Development and application of a 10 Hz Nd:YAG double pulse laser for vibration measurements with double pulse ESPI," In Fringe 2009, 1-6, Springer, Berlin (2009).
[17] Xie, X., Li, J., Zhang, B., Yan, L. and Yang, L., "Improvement of phase map quality for Michelson interferometer based spatial phase-shift digital shearography," Asian J. Phys. 24(10), 1391-1400 (2015).
[18] Anisimov, A. G., Serikova, M. G. and Groves, R. M. "3D shape shearography technique for surface strain measurement of free-form objects," Appl. Opt. 58(3), 498-508 (2019).
[19] Fällström, K-E., Gustavsson, H., Molin, N-E. and Wåhlin, A., "Transient bending waves in plates studied by hologram interferometry," Exp. Mech. 29(4), 378-387 (1989).
[20] Fällström, K-E., Lindgren, L-E. and Molin, N-E., "Transient bending waves in anisotropic plates studied by hologram interferometry," Exp. Mech. 29(4), 409-413 (1989).
[21] Wang, S., Dong, J., Pöller, F., Dong, X., Lu, M., Bilgeri, L.M., Jakobi, M., Salazar-Bloise, F. and Koch, A.W., "Dual-directional shearography based on a modified common-path configuration using spatial phase shift," Appl. Opt. 58(3), 593-603 (2019).